JOURNAL OF MATERIALS SCIENCE 24 (1989) 2250–2254

Crystal chemistry and magnetism in silicides $LaFe_{2-x}Rh_xSi_2$ ($ThCr_2Si_2$-type)

P. ROGL, K. HIEBL
Institut für Physikalische Chemie der Universität Wien, Währingerstraße 42, A-1090 Wien, Austria

G. WIESINGER
Institut für Experimentalphysik, Technische Universität Wien, Wiedner Hauptstraße 8-10, A-1040 Wien, Austria

A complete solid solution has been found for mixed crystals $LaFe_2Si_2$–$LaRh_2Si_2$ of the $ThCr_2Si_2$-type and a statistical distribution of iron- and rhodium atoms on the 4d sites of the space group I4/mmm. Crystal symmetry, atom order and precise atom parameters have been determined from a single crystal study of $LaFe_{1.6}Rh_{0.4}Si_2$ ($R = 0.015$).

Magnetic susceptibilities ($1.8 < T < 1100$ K) are characterized by a temperature independent paramagnetism throughout the solid solution. The iron atoms prove to be in a non-magnetic state in good agreement with Mössbauer data at 5 K and at room temperature, which further confirms a small amount of iron on a second crystallographic site (4e). $LaRh_2Si_2$ is not superconducting above 1.5 K.

1. Introduction

Despite much work [1–16] having been carried out on the structural chemistry and the physical properties of the $REFe_2Si_2$- as well as $LaRh_2Si_2$-compounds, many confusing results still remain.

Bodak and Gladyshevskij [1] were first to report the formation of $LaFe_2Si_2$ crystallizing with $ThCr_2Si_2$-type structure (X-ray powder data). Later Felner [2, 3] and Rossi [4] confirmed the existence of $ThCr_2Si_2$-type $LaFe_2Si_2$; they also reported resistivity and magnetic susceptibility data [2, 3] of $\mu_{eff} = 0.29\,\mu_B$ at 4.2 K and a weak ferromagnetic ordering at $T_m = 668(5)$ K. From magnetization and Mössbauer effect studies most of the iron (94%) was concluded to be diamagnetic [2]. More recent room temperature data, however, seemed to indicate only one type of iron atoms in the structure without a magnetic moment [5, 6].

Agreement exists about the formation and the crystal symmetry of $ThCr_2Si_2$-type $LaRh_2Si_2$ [7–14]; a type II superconducting transition was reported $T_c = 3.9$ K [8–10], however, was claimed to be due to the presence of superconducting neighbouring La–Rh–Si impurity phases [11–14]. Measurements of magnetization, a.c. susceptibility, electric resistivity and specific heat furthermore seemed to indicate a magnetic ordering at $T_m = 7$ K interpreted as itinerant electron long range order of the rhodium 4d electrons [9, 10]. From a very recent investigation of $La_{1+x}Rh_{2-y}Si_{2+y}$ alloys [13, 14] no indications for a magnetic transition were observed and from a.c. susceptibility data on a $LaRh_2Si_2$ single crystal type I superconductivity was found below 0.074 K [13].

In view of these conflicting results concerning both compounds $La(Fe, Rh)_2Si_2$, a closer inspection of the solid solution $LaFe_{2-x}Rh_xSi_2$ became the subject of the present work.

2. Experimental details

All samples were prepared by arc melting the high purity elements in a Ti/Zr-gettered argon atmosphere starting from a nominal composition La(20 at %), Fe + Rh(40), Si(40). Weight losses due to the arc melting process generally were less than 1 wt %. Filings of a lanthanum-ingot (99.9% pure, Rare Earths Products, Widnes, UK) and elemental powders of iron (99.9999% Puratronic, Johnson and Mattey and Co., UK), rhodium (99.9% Engelhard Ind., N.J. USA) and silicon (99.9999% Alpha Ventron, Karlsruhe, FRG) were used. Further details of sample preparation and heat treatments employed (600° C for 150 h, and at 800° C for 150 hrs), metallographic and X-ray techniques applied as well as a general description of the magnetic measurements (Faraday method) and the superconductivity measurements (a.c.-induction equipment) have been published elsewhere [15].

Mössbauer spectra were recorded with a standard constant acceleration type spectrometer and a source of 20 mCi ^{57}Co in a rhodium-matrix. The data were computer fitted by a least square procedure assuming a superposition of Lorentzian lines. Isomer shift values are given with respect to α-Fe at room temperature.

3. Results and discussion

3.1. The crystal structure of $LaFe_{1.6}Rh_{0.4}Si_2$ ($ThCr_2Si_2$-type)

A small single crystal specimen of $La(Fe_{0.8}Rh_{0.2})_2Si_2$

0022–2461/89 $03.00 + .12

TABLE I Crystallographic and magnetic data for the ternary silicides $LaFe_{2-x}Rh_xSi_2$ with the $ThCr_2Si_2$-type

Compound	Unit cell dimensions				μ_{eff} [μ_B]	T_c (K)	T_M (K)	References
	a (nm)	c (nm)	c/a (nm)	Vol (nm^3)				
$LaFe_{2.0}Si_{2.0}$	0.40523(6)	1.01532(20)	2.506	0.16673(6)	0.8		–	*
	0.406	1.015	2.500	0.16731	–		–	[5]
	0.4053	1.0153	2.505	0.16678	–		–	[4]
	0.4061	1.016	2.502	0.16657			668(5)	[2]
$LaFe_{1.8}Rh_{0.2}Si_2$	0.40681(9)	1.01317(38)	2.491	0.16768(9)				*
$LaFe_{1.6}Rh_{0.4}Si_2$	0.40818(3)	1.01225(41)	2.480	0.16865(12)				*
$LaFe_{1.5}Rh_{0.5}Si_2$	0.40884(9)	1.01129(36)	2.474	0.16904(10)	–		400, 750†	*
$LaFe_{1.4}Rh_{0.6}Si_2$	0.40958(5)	1.01250(12)	2.472	0.16985(5)				*
$LaFe_{1.2}Rh_{0.8}Si_2$	0.41028(9)	1.01350(50)	2.470	0.17060(11)				*
$LaFe_{1.0}Rh_{1.0}Si_2$	0.41087(8)	1.01509(17)	2.471	0.17136(8)				*
	0.41082(7)	1.01521(33)	2.471	0.17134(8)	–		420†	*
$LaFe_{0.8}Rh_{1.2}Si_2$	0.41087(7)	1.01769(50)	2.477	0.17180(10)				*
$LaFe_{0.6}Rh_{1.4}Si_2$	0.41098(5)	1.02120(56)	2.485	0.17248(10)				*
$LaFe_{0.5}Rh_{1.5}Si_2$	0.41150(8)	1.02300(23)	2.488	0.17294(8)				*
$LaFe_{0.4}Rh_{1.6}Si_2$	0.41121(4)	1.02371(59)	2.490	0.17310(11)	–		410†	*
$LaFe_{0.2}Rh_{1.8}Si_2$	0.41131(7)	1.02752(69)	2.498	0.17383(13)				*
$LaRh_{2.0}Si_{2.0}$	0.41107(8)	1.02927(47)	2.504	0.17392(11)	0.27	–	–	*
	0.4092	1.020?	2.493	0.17079	–	–	–	[7]
	0.4114(2)	1.031 (1)	2.506	0.17450	2.0	3.8	–	[9, 10]
	0.41109(8)	1.0289 (3)	2.503	0.17388	–	–	–	[12]
	0.4092	1.020	2.493	0.17079	–	3.90	–	[8]
	0.4112	1.029	2.502	0.1740	–	0.074	–	[13]

*This work.

† Ferromagnetism is strongly reduced or disappears upon annealing.

suitable for X-ray diffraction was obtained by mechanical fragmentation of an arc melted alloy with the nominal composition 20 at % La–32 at % Fe–8 at % Rh–40 at % Si, after annealing at 800° C. X-ray Laue and rotation photographs along the c-axis [0 0 1] confirmed the high Laue symmetry 4/mmm. Furthermore, heavily exposed photographs did not reveal any significant indications of superstructure formation. Indexing of the rotation and Guinier powder photographs was complete on the basis of a body-centred tetragonal unit cell suggesting isotypism with a $ThCr_2Si_2$-type structure. Lattice parameters and intensities of the single crystal fragment were measured with graphite monochromatized MoKα radiation on a STOE (Siemens) automatic four circle diffractometer. The crystallographic data are summarized in Table II. A total number of 785 reflections was recorded up to a limit of $\sin\theta/\lambda = 8.1\,\text{nm}^{-1}$. A set of 139 symmetry independent intensities was obtained by averaging "centred reflections" only, and all observed intensities (131 for which $|F_0| > 2\sigma$) were used in the structure refinement. An empirical absorption correction was applied using ψ scans of three independent reflections. With respect to the $ThCr_2Si_2$-type, refinement was performed in centrosymmetric I4/mmm employing the STRUCSY full matrix least squares system (STOE and CIE, Darmstadt). The weights used were $\omega_i = 1/[\sigma(F_i)]^2$; different weighting schemes had no significant influence on the R values obtained. The refinement in the $ThCr_2Si_2$-type (see Table II) unambiguously revealed a statistical occupation of iron and rhodium atoms in the 4d sites. Substitution of silicon atoms by iron was also investigated – it is interesting to note that the R value remained practically unaffected on replacement of silicon by iron up to 10% iron in the 4e sites. The final atom parameters, employing anisotropic thermal factors and correction of isotropic secondary extinction, are listed in Table II; interatomic distances up to 0.4 nm are shown in Table III.

3.2. The solid solution $LaFe_{2-x}Rh_xSi_2$

X-ray analysis of about 10 pseudobinary samples $LaFe_{2-x}Rh_xSi_2$ in the as-cast and the sintered condition revealed (a) a general congruent melting behaviour as well as (b) a complete solid solubility throughout the pseudobinary system for $T < 600°$ C. Guinier

TABLE II Atomic and thermal parameters for $ThCr_2Si_2$-type $La(Fe_{0.8}Rh_{0.2})_2Si_2$

Atom	Site	x	y	z	occ.	$U_{equiv.}$	U_{11}	U_{22}	U_{33}
La	2a	0	0	0	1.000	0.0082	0.0081(2)	0.0081(2)	0.0085(2)
Fe }	4d	0	1/2	1/4	0.797(6)	0.0071	0.0072(2)	0.0072(2)	0.0069(3)
Rh }	4d	0	1/2	1/4	0.203(6)	0.0071	0.0072(–)	0.0072(–)	0.0069(–)
Si†	4e	0	0	0.3667(2)	1.000	0.0096	0.0091(4)	0.0091(4)	0.0107(6)

Space group: I4/mmm, D_{4h}^{17} – No. 139; origin at $\bar{1}$, $Z = 2$;
$a = 0.40827(1)$ nm, $c = 1.01211(6)$ nm, $V = 0.1687\,\text{nm}^3$; $D_x = 6.50\,\text{Mg m}^{-3}$, μ (MoKα) $= 20.49\,\text{mm}^{-1}$
Standard deviations are in parentheses; $R = 0.015$, $R_w = 0.015$.
Isotropic temperature factors are expressed as: $T = \exp[-2\pi^2 \times 10^{-2}\, U(2\sin\theta/\lambda)^2]$; anisotropic thermal factors are the form: $T = \exp[-2\pi(U_{11}h^2a^{*2} + U_{22}k^2b^{*2} + U_{33}l^2c^{*2} + 2U_{12}hka^*b^* + \ldots)10^{-2}]$, by symmetry $U_{12} = U_{13} = U_{23} = 0$. Correction for isotropic secondary extinction was 1.8×10^{-6}.

†Substitution of up to maximal 10% of silicon by iron in the 4e-sites does not change the R value significantly.

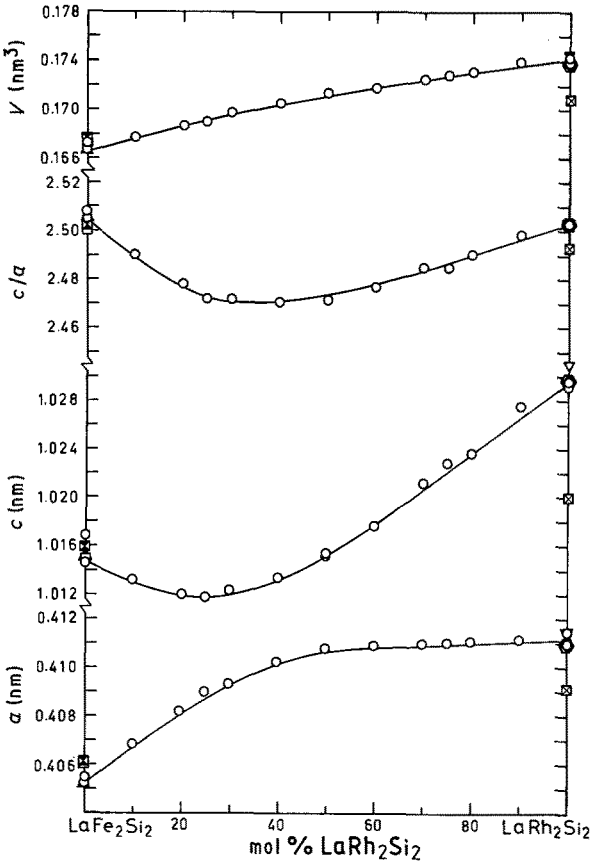

Figure 1 Lattice parameters and unit cell volumes of the ternary alloys $LaFe_{2-x}Rh_xSi_2$ with $ThCr_2Si_2$-type structure. (○ this work, ⊠ [3], ⊠ [7], △ [4], □ [5], ▽ [9], ◇ [12], ○ [14]).

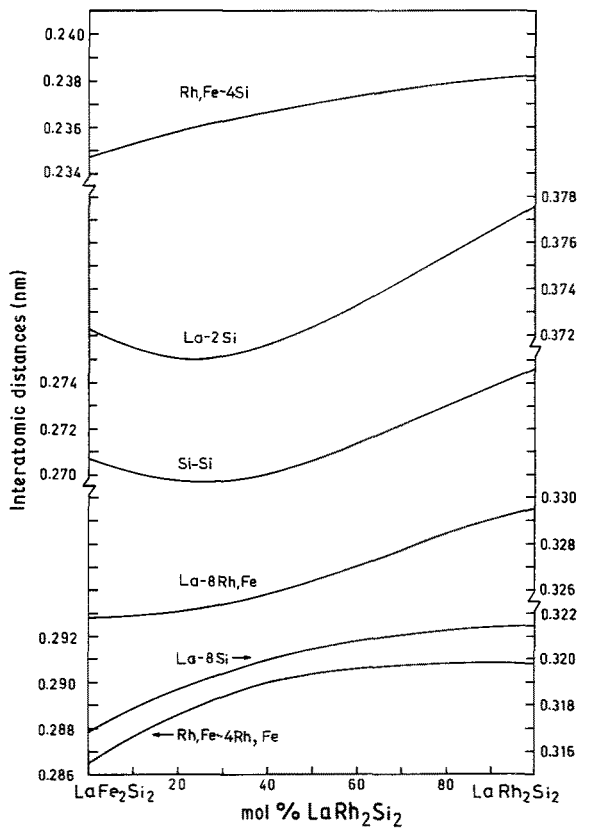

Figure 2 Variation of interatomic distances in $LaFe_{2-x}Rh_xSi_2$ as a function of the Fe–Rh exchange. Atom parameters used are taken from Table II.

powder patterns were indexed completely on the basis of a body centred tetragonal unit cell (see Table I) and thereby indicate $ThCr_2Si_2$-type structural analogy. By use of the atom order and atom parameters as derived from the single crystal study of $LaFe_{1.6}Rh_{0.4}Si_2$ the observed and calculated X-ray powder intensities for all the alloys $LaFe_{2-x}Rh_xSi_2$ are found to be in excellent agreement. Fig. 1 represents the variation of the lattice parameters and volumes for the pseudobinary section $LaFe_{2-x}Rh_xSi_2$ as a function of the iron–rhodium exchange. Whereas the variation of the volume within the solid solution seems to reflect the general mixing behaviour with a slight positive deviation from Vegard's rule, the variation of the individual unit cell dimensions (u.c.d.) on Fe–Rh-substitution reveals an initially rather steep (< 40 mol %) but later flat increase of the *a*, *b* parameters compensated by an initially decreasing *c* parameter changing its slope above 25 mol % $LaRh_2Si_2$. This puzzling behaviour might be explained on the basis of a recent analysis of the u.c.d.s in $BaAl_4$-type phases in terms of nearest-neighbour diagrams [16]: according to this analysis [16] the u.c.d.s in $REFe_2Si_2$-phases are mainly controlled by the RE–Si distances whereas the RE–Rh contacts exert a dominant control in the $RERh_2Si_2$-phases. On insertion of rhodium into the iron sublattice of $LaFe_{2-x}Rh_xSi_2$ the initially steep increase of the *a* axis thus forces an inflection in the dependency of the *c* axis with the Fe–Rh substitution.

3.3. Magnetic behaviour and superconductivity

The magnetic behaviour of $LaRh_2Si_2$ is characterized by a temperature independent Pauli paramagnetism due to the metallic state. At temperatures below 20 K a small Curie-tail appears, which is rather attributed to a contamination by magnetic RE-impurities ($< 1\%$) than to a magnetic moment on the lanthanum itself. A calculation according to a modified Curie–Weiss law, leads to a small moment of $\mu_{eff} = 0.27\,\mu_B$ per formula unit. In contradiction to earlier findings [9, 10] we do not find any hint for the onset of long range ferromagnetic ordering of the rhodium sublattice.

Partial substitution of the rhodium atoms by iron gives rise to a weak ferromagnetism with varying

TABLE III Interatomic Distances in $La(Fe_{0.8}Rh_{0.2})_2Si_2$ less than < 0.4 nm

La – 8 (Fe, Rh)*	0.3251			(Fe, Rh)* – 4 La	0.3251
– 8 Si	0.3186			– 4 (Fe, Rh)*	0.2887
– 2 Si	0.3711			– 4 Si	0.2359
		Si – 1 La	0.3711		
		– 4 La	0.3186		
		– 4 (Fe, Rh)*	0.2359		
		– 1 Si	0.2698		

*(Fe, Rh) represents a statistical distribution of 3.188 Fe + 0.812 Rh in the 4d sites.

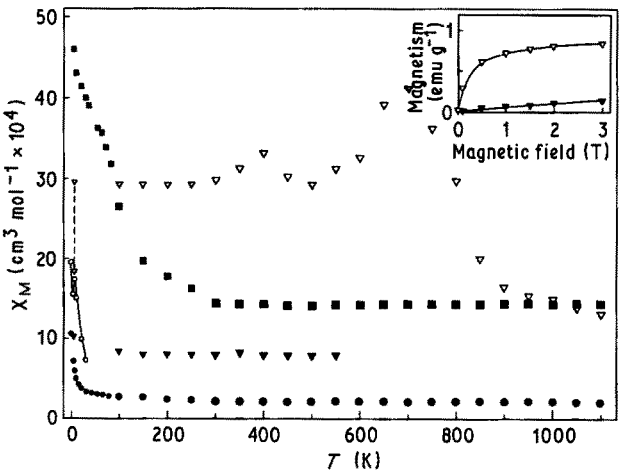

Figure 3 Molar susceptibility plotted against temperature for $LaFe_{2-x}Rh_xSi_2$, x = 0, 1, 2. (■ $LaFe_2Si_2$, ▽ $LaFe_{1.5}Rh_{0.5}Si_2$ arc., ▼ $LaFe_{1.5}Rh_{0.5}Si_2$ ann. ● $LaRh_2Si_2$, ○ [9]).

onset temperatures (see Table I). However, a calculation of the saturation moment σ at 5 K (see Fig. 3) results in very small values, i.e. $0.027 < \sigma < 0.07\,\mu_B$. Heat treatment of the alloys generally leads to a reduction of the moments by a factor of 10, supporting the assumption that the ferromagnetic ordering is not a bulk phase property (see also Mössbauer data). A Honda–Owen extrapolation of the susceptibility data at 5 K and high fields (2 to 3 T) confirms that the magnetism of the whole solid solutions remains temperature independent. The maximum susceptibility stems simply from extrapolated data passing the ferromagnetic transition of the secondary phases.

In the pure $LaFe_2Si_2$ alloy the iron again proves to be in a non-magnetic configuration (d^{10} ?) above room temperature. However, upon lowering the temperature the susceptibility becomes Curie-like. A least squares calculation resulted in a moment $\mu_{eff} = 0.8\,\mu_B$ per iron atom (without any correction for additional contributions from RE-impurities), confirming some tendency of moment formation at the iron site, due to a partial localization of the 3d electrons. No magnetic ordering was encountered down to 1.5 K.

In contradiction to earlier data [9, 10], but in agreement with Palstra *et al.* [13] $LaRh_2Si_2$ does not undergo a superconducting transition above 1.5 K.

TABLE IV Quadrupole splitting, isomer shift S and line width Γ originating from the Fe 4d atoms in $La(Rh_xFe_{1-x})_2Si_2$; in mm sec^{-1} ± 0.01

x	$e^2qQ/2$	S (rel.α-Fe)	Γ
T = 5 K			
0	0.08	0.46	0.30
0.25	0.17	0.56	0.38
0.5	0.16	0.43	0.34
0.75	0.15	0.36	0.35
T = 300 K			
0	0.04	0.21	0.29
0.25	0.11	0.22	0.27
0.5	0.14	0.24	0.29
0.75	0.14	0.25	0.27

3.4. ^{57}Fe Mössbauer spectroscopy

The Mössbauer spectra recorded at room- and liquid helium temperature were of a slightly asymmetric shape, thus revealing a small amount (10 to 15%) of

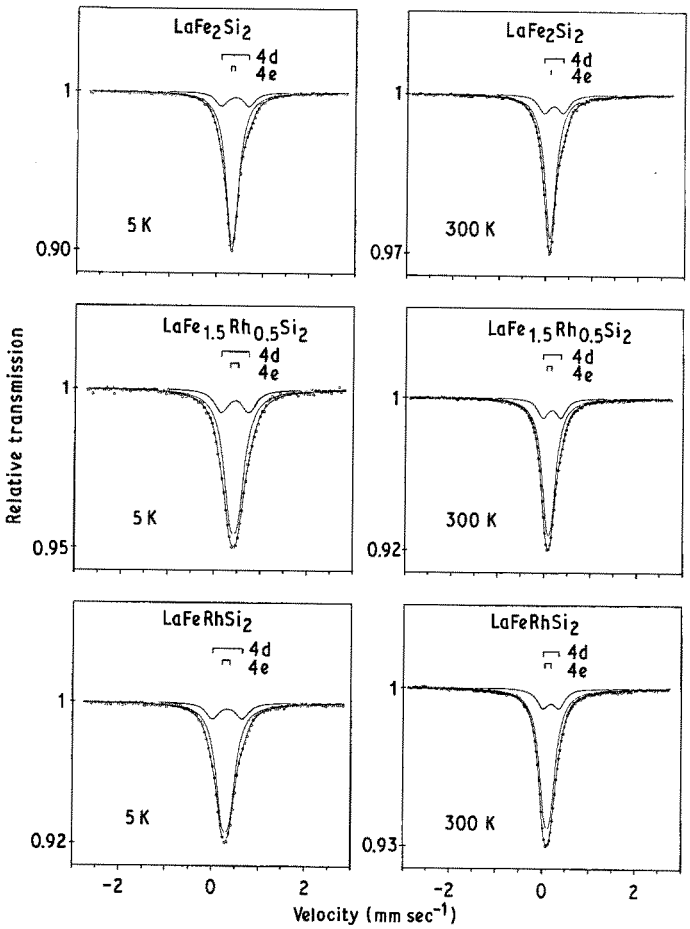

Figure 4 Mössbauer spectra of $LaFe_{2-x}Rh_xSi_2$, experimental data ●, calculated profile; the solid bars indicate the Fe-contributions from the different iron-sublattice sites i.e. 4Fe in (4d) and 0.4 Fe in (4e).

non-magnetic iron on a second site (4e) (Fig. 4). Consequently the data were analysed by superimposing two doublets with equal line width. As the resulting hyperfine parameters originating from the weak pattern are accompanied with a larger uncertainty, only those derived from the main subspectrum (4d sites, Table IV) have been used in the discussion below.

The main component showed only a small quadrupole splitting, thus representing the highly symmetric environment of the Mössbauer atom located at the 4d sites. The splitting of the weak doublet was distinctly larger, indicating an iron site with an appreciable non-zero electric field gradient which may be caused by the lower symmetry and a stronger Fe–Fe interaction at the 4e sites. The isomer shift of the weak pattern was found to exceed that of the large one by less than $+0.1\,\mathrm{mm\,sec^{-1}}$ pointing to a slightly smaller s-(higher d-) electron density for iron at the silicon sites.

The observation of a second quadrupole pattern for these compounds is in contradiction with the results obtained by Umarji *et al.* [5], who observed for $LaFe_2Si_2$ a broadened, however, symmetric single line spectrum with a quadrupole splitting which is five times larger than that observed for the main component in the present case (see Table II in [5]). The reason for the occurrence of an asymmetric line shape in certain cases lies to our opinion in differences in the sample preparation, particularly in the annealing procedure. The question, if the second hyperfine pattern is due to an impurity phase can not be decided from Mössbauer effect measurements. However, the intensity deduced from the Mössbauer data ($\sim 10\%$) should easily be visible in an X-ray diffraction diagram and thus the possibility of the occupation of iron on a second lattice site is favoured.

It is worthwhile studying the hyperfine parameters as a function of the rhodium concentration and temperature (Table IV). The line width does not vary significantly with the amount of rhodium; the increase at low temperatures is commonly observed and may be due to temperature induced lattice distortions. The rise of $\Gamma = 0.02\,\mathrm{mm\,sec^{-1}}$ between room and liquid helium temperature observed in the case of pure $LaFe_2Si_2$ is surprisingly small. The quadrupole splitting increases with growing amounts of rhodium up to concentrations $x \sim 0.5$, from where it stays almost constant independent of temperature. At room temperature the isomer shift values increase only slightly with the concentration which is no longer the case at low temperatures. There a distinctly non-uniform behaviour is obtained, showing a maximum at $x = 0.25$. A comparison of the quadrupole splitting at $T = 300\,\mathrm{K}$ with that obtained at $T = 5\,\mathrm{K}$ shows a pronounced decrease in the rise with increasing rhodium concentration, revealing a weakening of the temperature dependence of the quadrupole interaction with increasing rhodium concentration. At high rhodium concentrations the quadrupole interaction is essentially independent of temperature. The total quadrupole splitting can be built up from a lattice contribution and a valence electron contribution each exhibiting its specific temperature dependence. A temperature independence, as observed in the case of the rhodium-rich compounds has thus to be attributed to an inverse temperature behaviour of the two quadrupole contributions.

The temperature induced rise in isomer shift $\Delta S = (S(5\,\mathrm{K})\text{-}S(3.00\,\mathrm{K}))$ is also reduced significantly with the amount of rhodium. In both cases – $\Delta(\Delta E_Q)$ and ΔS – a maximum is obtained at $x = 0.25$ which should be compared with the minimum found for the lattice parameter c and the ratio c/a for almost the same concentration (Fig. 1). This agreement is reasonable, as the isomer shift shows a tendency to more positive values (smaller s-electron density) with increasing volume of the atomic cell.

Acknowledgements

The investigation was supported by the Austrian Science Foundation (Fonds zur Förderung der wissenschaftlichen Forschung in Österreich) through grant No. 5297. The financial support for the Guinier–Huber equipment by the foundation "600 Jahre Wiener Universität" is gratefully acnowledged. P.R. expresses his gratitude to the Hochschuljubiläumsstiftung der Stadt Wien for the KD-530 type microdensitometer and the MNT-306 microbalance. Thanks are also due to the Austrian Science Foundation for the use of the SUS-10.

References

1. O. I. BODAK and E. I. GLADYSHEVSKIJ, *Vestnik, Lvov. Derzh. Univ. Ser. Khim.* **14** (1972) 29.
2. I. FELNER, I. MAYER, A. GRILL and M. SCHIEBER, *Solid State Commun.* **16** (1975) 1005.
3. I. FELNER and I. MAYER, *Mater. Res. Bull.* **8** (1973) 1317.
4. D. ROSSI, R. MARAZZA and F. FERRO, *J. Less C. Metals* **58** (1978) 203.
5. A. M. UMARJI, D. R. NOAKES, P. J. VICCARO, G. K. SHENOY, A. T. ALDRED and D. NIARCHOS, *J. Magn. Magn. Mater.* **36** (1983) 61.
6. D. R. NOAKES, A. M. UMARJI and G. K. SHENOY, *ibid.* **39** (1983) 309.
7. R. BALLESTRACCI, *C.R. Acad. Sci. Paris* **B282** (1976) 291.
8. B. CHEVALIER, P. LEJAY, M. VLASSE, J. ETOURNEAU and P. HAGENMULLER, *Mater. Res. Bull.* **17, 1211, 18** (1983) 315.
9. I. FELNER and I. NOWIK, *Solid State Commun.* **47** (1983) 831.
10. *Idem., J. Phys. Chem. Solids* **45** (1984) 419.
11. H. F. BRAUN, *J. Less Common Met.* **100** (1984) 105.
12. R. N. SHELTON, H. F. BRAUN and E. MUSICK, *Solid State Commun.* **52** (1984) 797.
13. T. T. M. PALSTRA, G. LU, A. A. MENOVSKY, G. J. NIEUWENHUYS, P. H. KES and J. A. MYDOSH, *Phys. Rev.* **B34** (1986) 4566.
14. T. T. M. PALSTRA, Thesis, Reiksuniversiteit te Leiden (1986).
15. K. HIEBL, C. HORVATH, P. ROGL and M. J. SIENKO, *J. Magn. Magn. Mater.* **37** (1983) 287.
16. W. PEARSON and P. VILLARS, *J. Less Common Met.* **97** (1984) 119, 133, 141.

Received 18 March
and accepted 28 July 1988